New Phytologist Supporting Information

Article title: Home-based microbial solution to boost crop growth in low-fertility soil

Authors: Meitong Jiang, Delgado-Baquerizo Manuel, Mengting Maggie Yuan, Jixian Ding, Etienne Yergeau, Jizhong Zhou, Thomas W. Crowther, Yuting Liang

Article acceptance date: 4-April-2023

Supplementary Figures

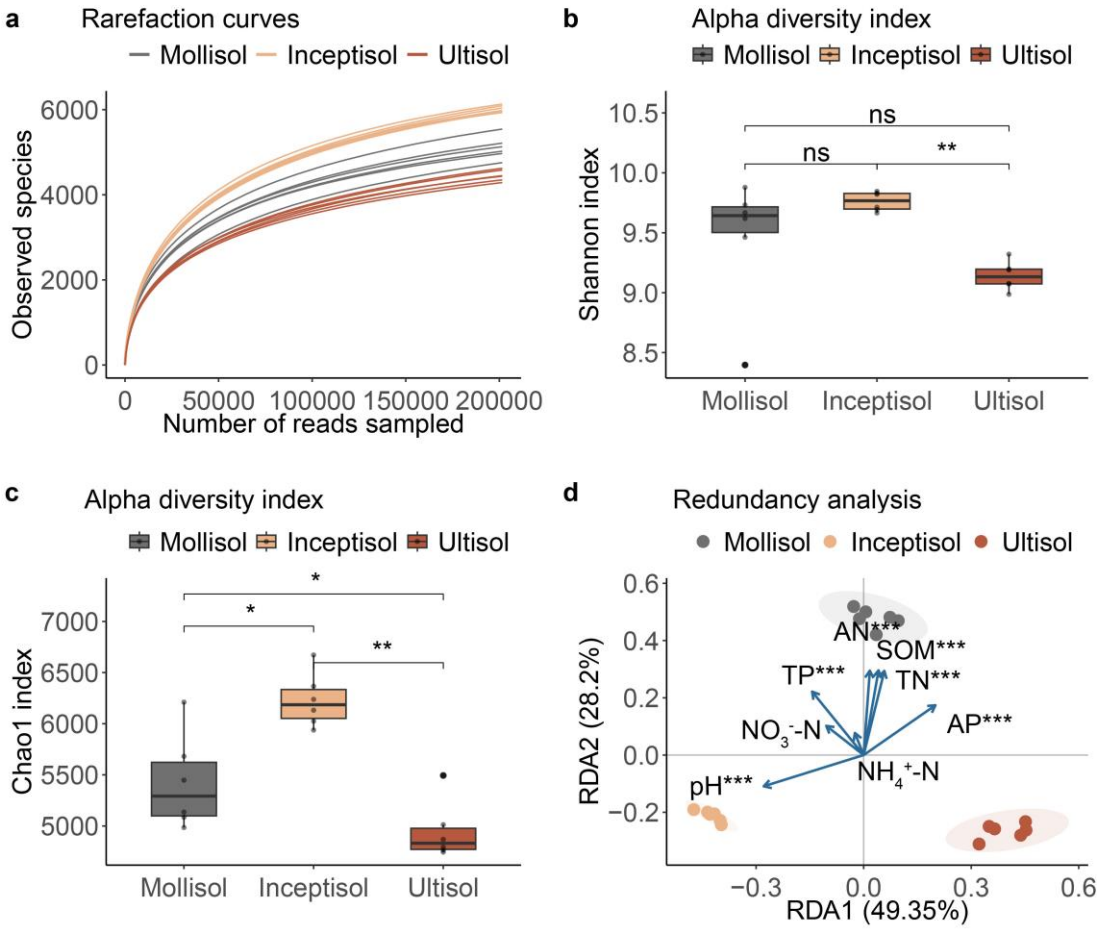

Figure S1 Alpha and beta diversity of rhizosphere microbial communities in Mollisol, Inceptisol and Ultisol. a Rarefaction curves, **b** Shannon**,** and **c** Chao1 indexes of original field rhizosphere soil samples in Mollisol, Inceptisol and Ultisol, respectively. Statistical analyses were performed by a paired Wilcoxon rank-sum test (* indicates $P < 0.05$, ** indicates $P < 0.01$, *** indicates $P < 0.001$). In all box plots, the horizontal bars represent medians. The tops and bottoms of the boxes show the 75th

and 25th percentiles, respectively. n = 6 rhizosphere soil samples were measured. Nonsignificant differences are labeled ns. **d** Redundancy analysis revealed that soil type was a major source of bacterial community variation. Each point corresponds to a different sample colored by soil type. SOM, soil organic matter; TN, total N; TP, total P; AN, available N; AP, available P.

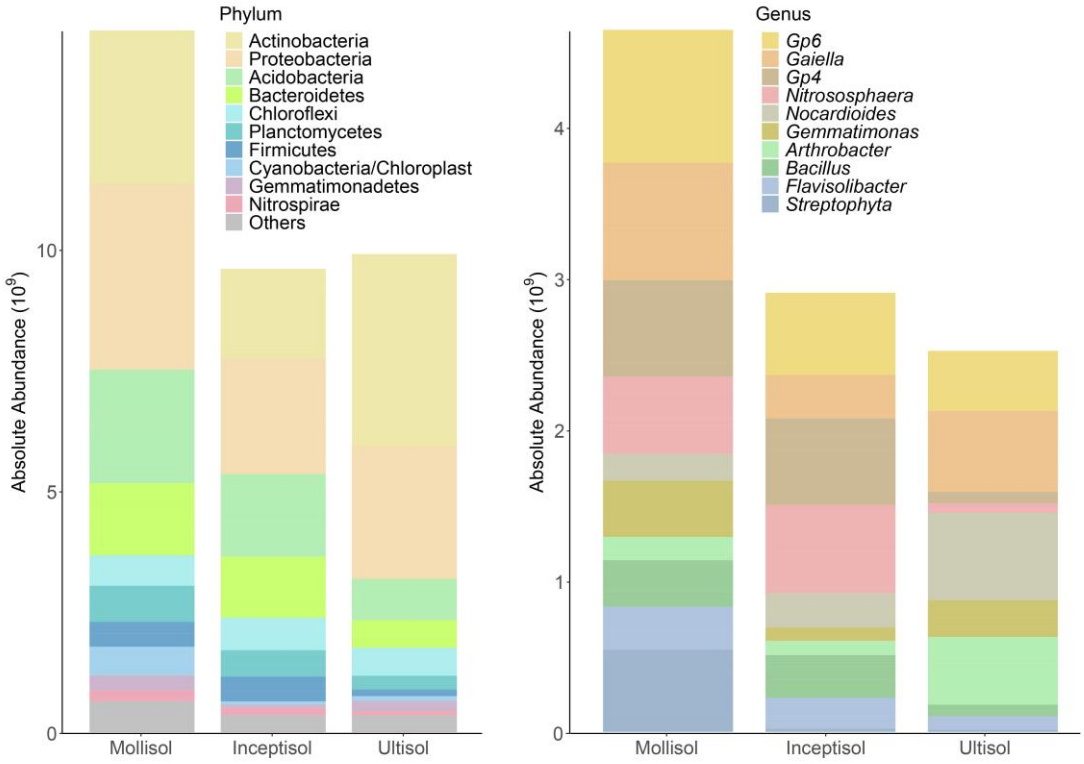

Figure S2 Absolute quantification of 16S rRNA to reveal rhizosphere microbial community composition. Top 10 bacterial taxa at **a** phylum and **b** genera level in field rhizosphere soil samples from Mollisol, Inceptisol and Ultisol.

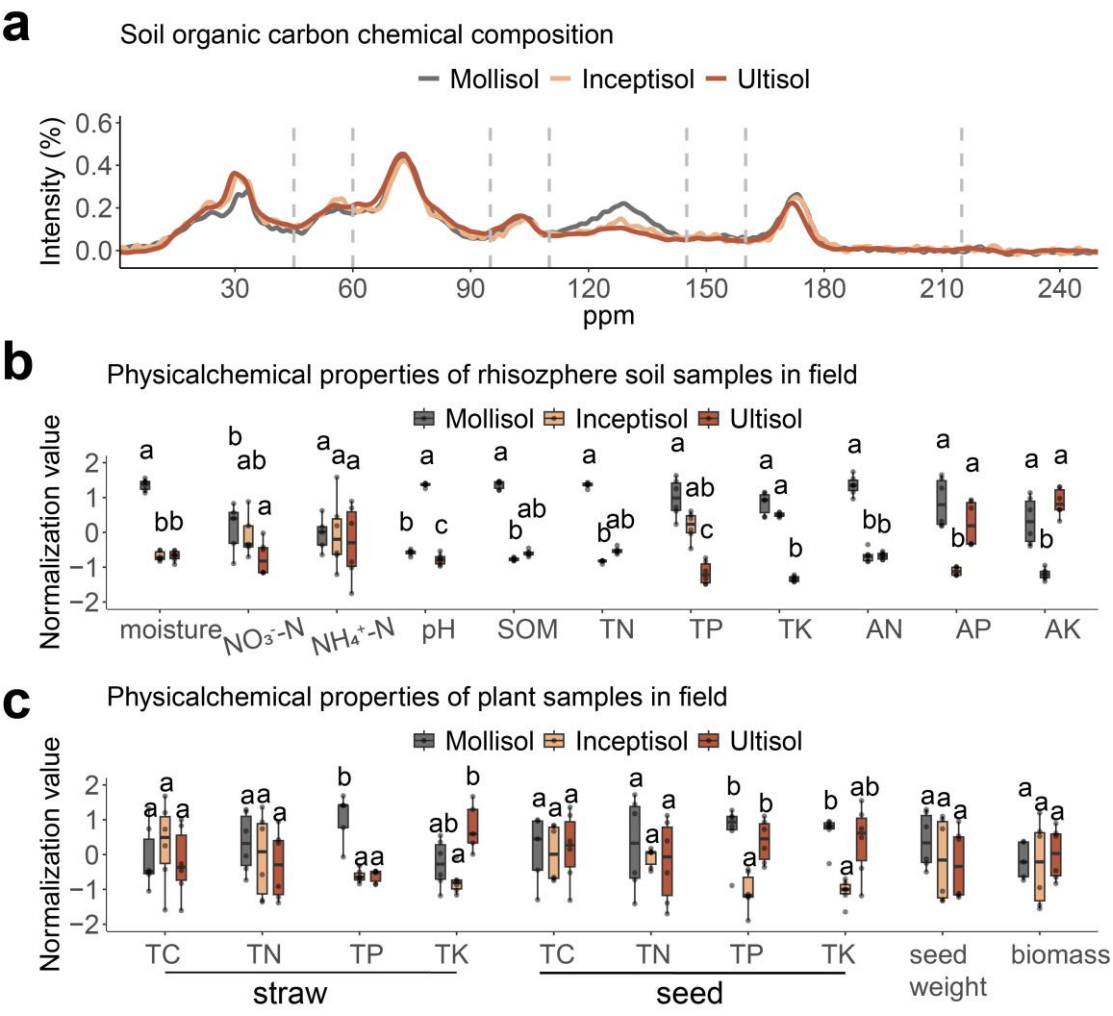

Figure S3 Physicochemical properties of environmental samples in the field. a Chemical structure of organic carbon in soils. Labile carbon components are indicated in bold. **b** and **c** Physicochemical properties of **b** rhizosphere soil and **c** plant samples. SOM, soil organic matter; TN, total N; TP, total P; TK, total K; AN, available N; AP, available P; AK, available K; TC, total carbon. n = 6 rhizosphere soil samples and plant samples were measured. The different letters in **b** and **c** indicate significant differences ($P < 0.05$) using multiple comparisons of nonparametric tests (Nemenyi test). In box plots, the horizontal bars represent medians. The tops and bottoms of the boxes show the 75th and 25th percentiles, respectively.

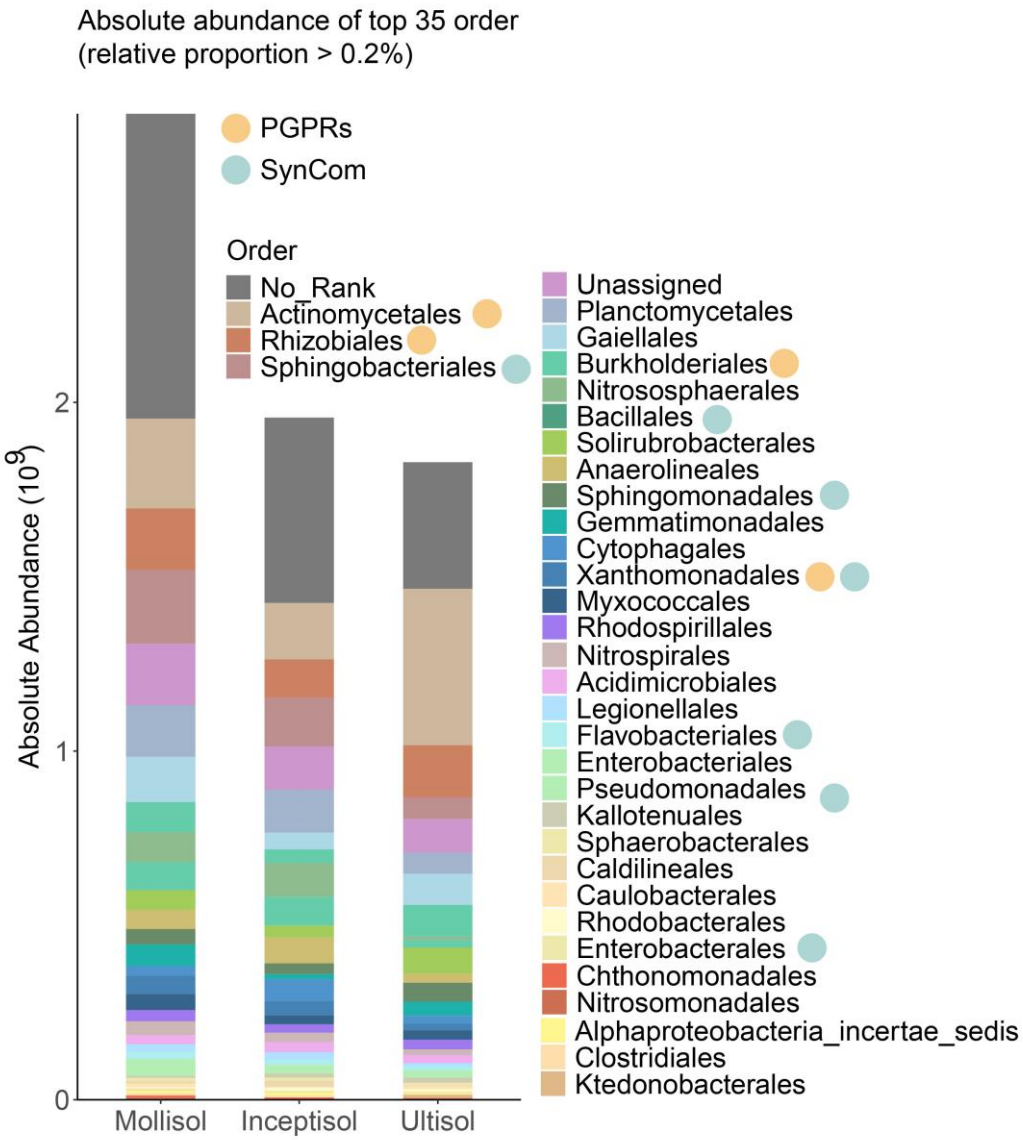

Figure S4 The 21 species of SynCom and 4 strains of PGPR belonged to the most abundant taxa at the order level. Absolute abundance of the top 35 orders. Colored circles alongside the order refer to the SynCom or PGPRs to which they belonged.

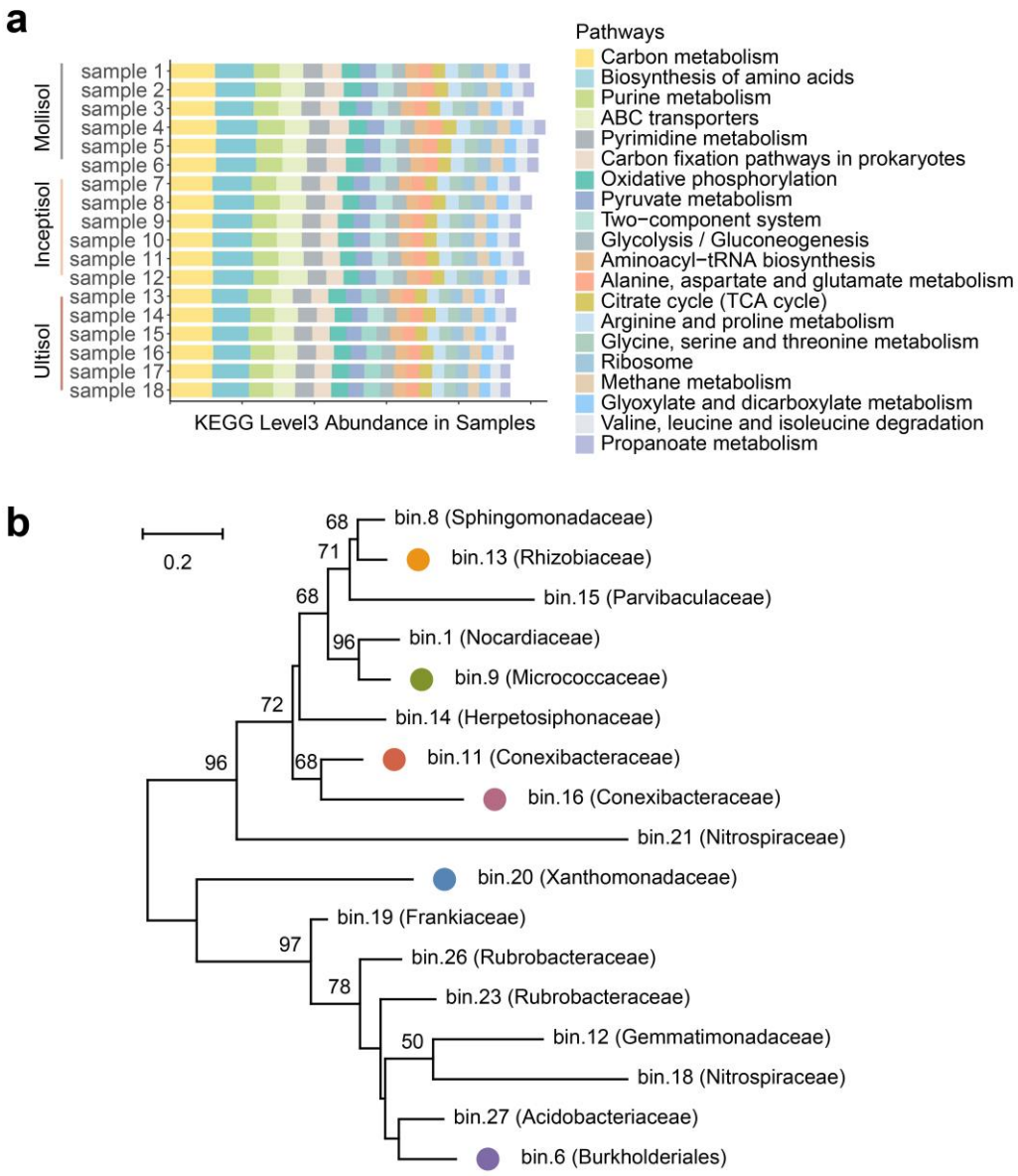

Figure S5 Metagenomic binning and functional clustering. a Metagenomic functional clustering of KEGG results based on Bray–Curtis distance. The KO (KEGG orthology) abundance of each group was obtained from the KEGG database at level 3. **b** Phylogenetic relationship among bins (completeness > 50%, contamination < 10%) using *rpoD* sequences. Five genomes (bin. 2, bin. 7, bin. 17, bin. 22 and bin. 25) were not included due to the absence of the *rpoD* gene, as the genomes were incomplete. The colored dots indicate that the contamination rate of assembled genomes was lower than 5%. The phylogram was constructed using the NJ method. Bootstrap values > 50 are shown.

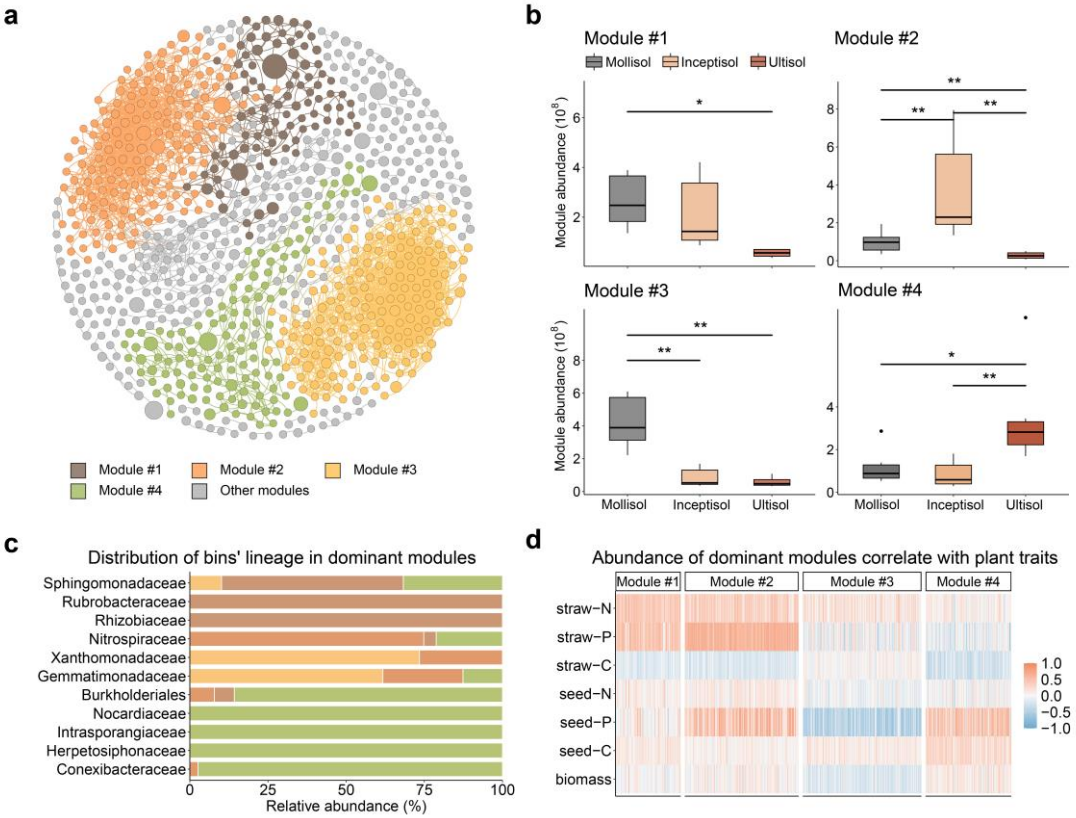

Figure S6 Association of microbial network modules, metagenome bins and plant traits. a Co-occurrence network based on Pearson correlations constructed using the random matrix theory (RMT)-based network approach. Data were obtained by absolute quantitative sequencing. The sizes of the nodes represent their abundance, and the different colors represent different modules. **b** Abundance of modules in different soils. The Wilcoxon test was used to evaluate the significance of differences (* indicates $P < 0.05$; ** indicates $P < 0.01$; *** indicates $P < 0.001$). Nonsignificant differences were not marked. n = 6 for each soil. **c** Distribution of bins' lineages in dominant modules. **d** Heatmap of Spearman's rank correlation values between the absolute abundance of species in dominant network modules and plant traits.

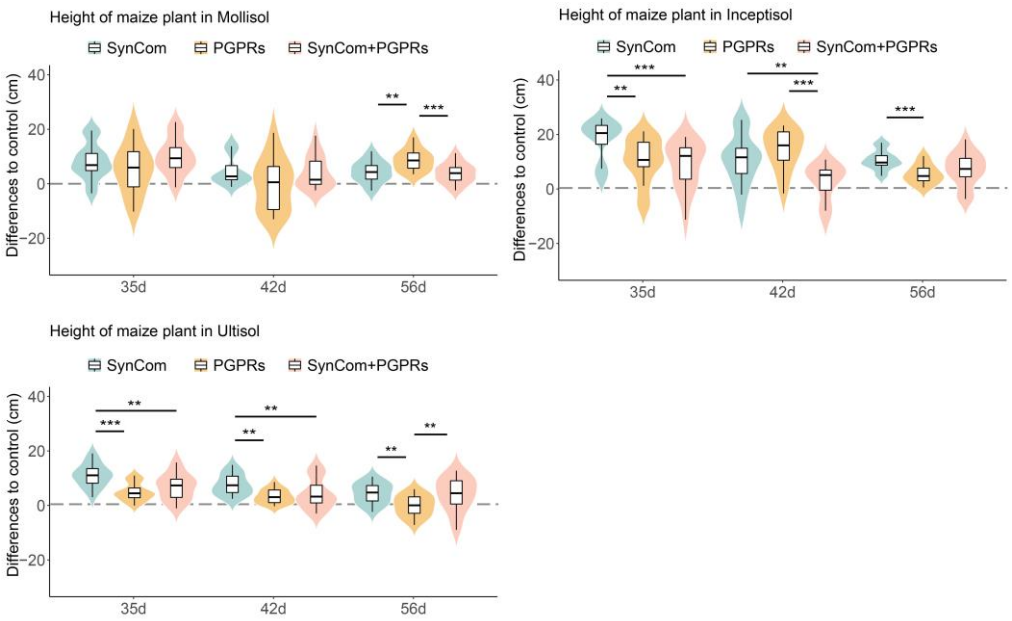

Figure S7 Comparison of plant height of maize plants between the treatment and control groups at 35 days (V4-V5 stage), 42 days (V5-V6) and 56 days (V7-V8 stage). The Wilcoxon test was used to determine significance (* indicates $p < 0.05$; ** indicates $p < 0.01$; *** indicates $p < 0.001$). Nonsignificant differences were not labeled. n = 4 for each treatment.

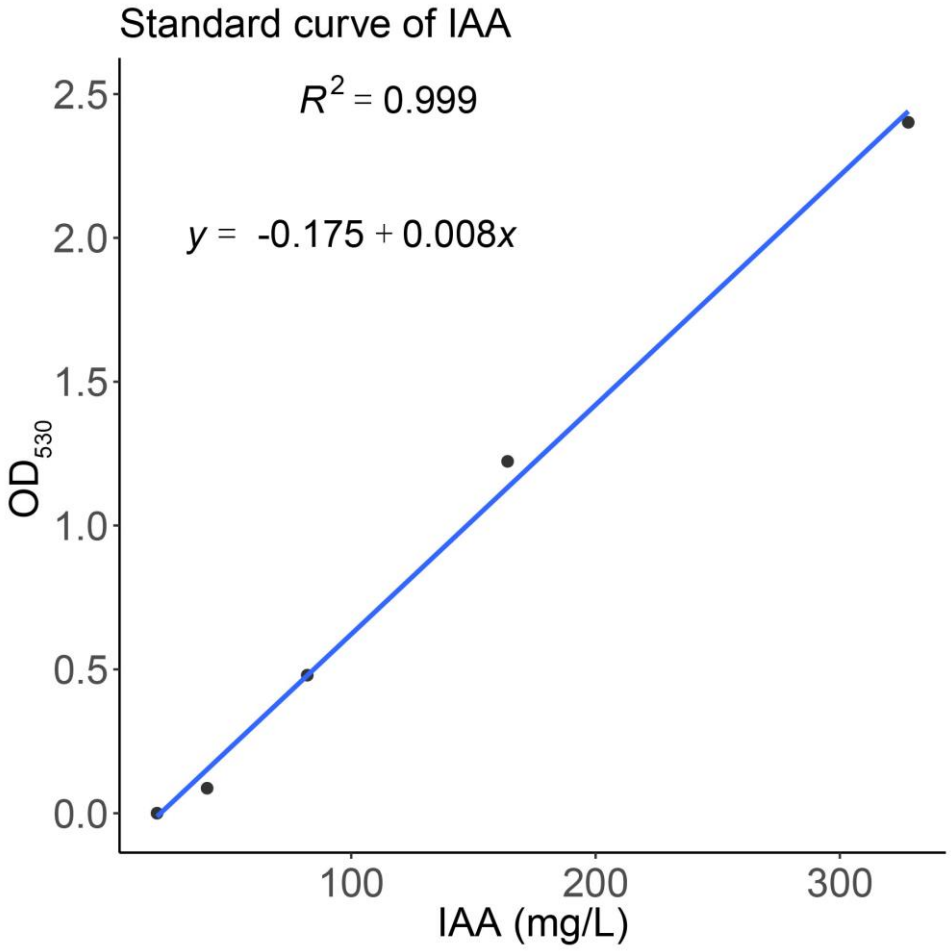

Figure S8 The standard curve of IAA content in suspension. IAA: indole acetic acid.

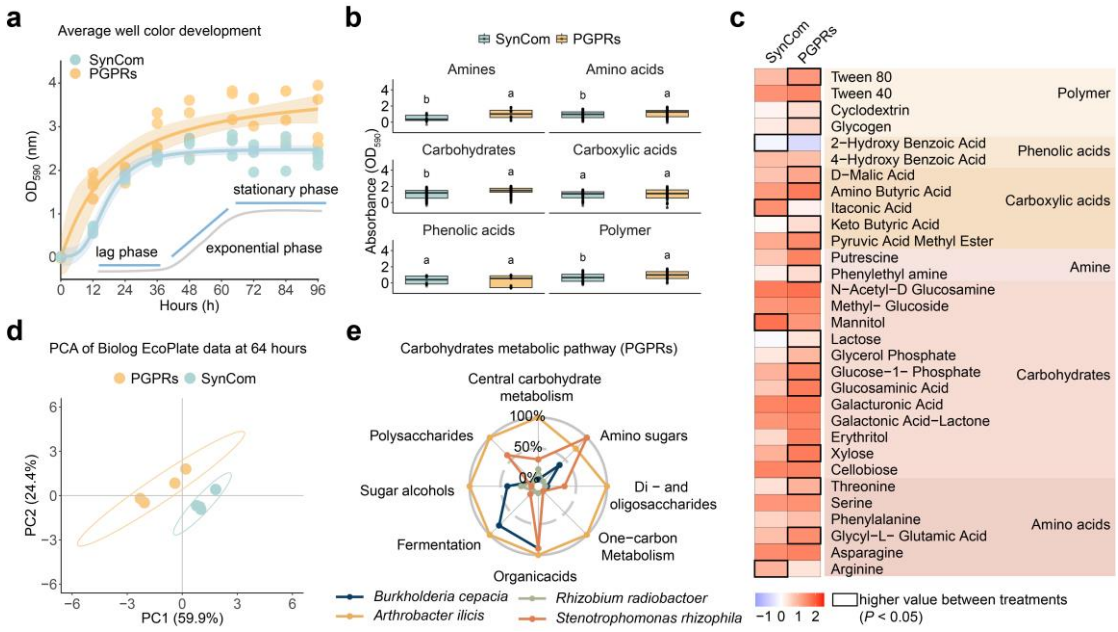

Figure S9 Metabolic diversity of carbon sources. a Changes in average well color development (AWCD) of microbial inoculants over 95 hours on a Biolog EcoPlate. The curve was fitted by the logistic model $y = A_2 + \frac{A_1 - A_2}{1 + \left(\frac{x}{x_0}\right)^p}$, A1: initial value, A2: final value, x0: time of the maximum growth rate, p: the maximum growth rate). **b** and **c** The utilization capacity of carbon sources in different microbial inoculants. The different letters in **b** indicate significant differences ($P < 0.05$) using multiple comparisons of nonparametric tests (Nemenyi test). In box plots, the horizontal bars represent medians. The tops and bottoms of the boxes show the 75th and 25th percentiles, respectively. **d** Carbon metabolic preference of microbial inoculants was determined after 64 hours of incubation on a Biolog EcoPlate. For each carbon source, n = 3 replicates in Biolog plates. For each treatment, n = 4 replicates of Biolog plates. **e** Potential ability to utilize carbohydrates inferred by the related functional genes in the representative genomes of the four PGPRs.

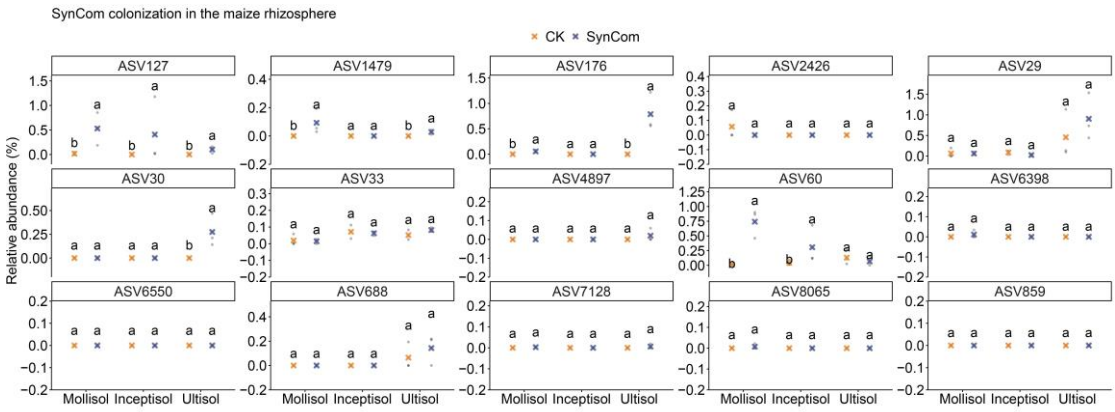

Figure S10 Relative abundances of the bacterial ASVs matched to SynCom members in the maize rhizosphere grown in the greenhouse. Information on ASVs and corresponding species is shown in Table S4. The relative abundances of the three replicates are shaded as gray dots, and the mean is shown as a cross with the color referring to the treatment. The different letters indicate significant differences ($P < 0.05$) using multiple comparisons of nonparametric tests (Nemenyi test).

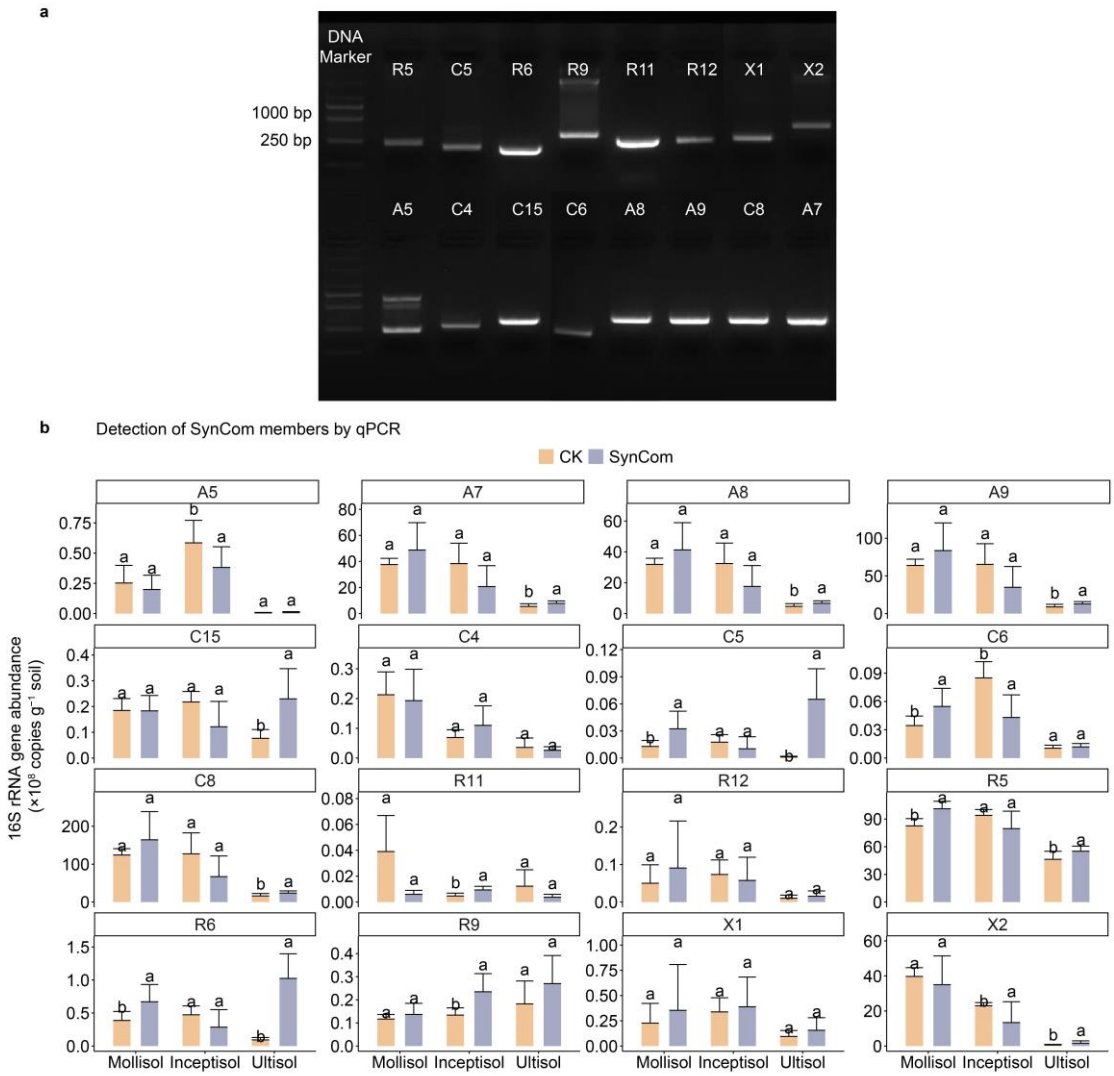

Figure S11 Detection of SynCom members by qPCR. a Denaturing gradient gel electrophoresis (DGGE) analyses of 16S rRNA gene fragments showed the specificity of primers for the monoculture of each strain. **b** Histogram showing the 16S rRNA gene abundance in real-time PCR by eleven primers. The different letters indicate significant differences ($P < 0.05$) using the Wilcoxon test. The error bar represents the sd. n = 3. *A5*, *Stenotrophomonas rhizophila;* A8, *Pantoea vagans*; A7, *Serratia marcescens;* A9, *Citrobacter farmer*; C15, *Acinetobacter pittii*; C4, *Pseudomonas mosselii*; C5, *Enterobacter cancerogenus*; C6, *Lysinibacillus macrolides*; C8, *Enterobacter hormaechei subsp. steigerwaltii*; R11, *Chryseobacterium cucumeris*; R12, *Stenotrophomonas maltophilia*; R5, *Bacillus cereus*; R6, *Enterobacter ludwigii*; R9, *Pseudomonas koreensis*; X1, *Pseudomonas geniculate*; X2, *Sphingomonas desiccabilis*.

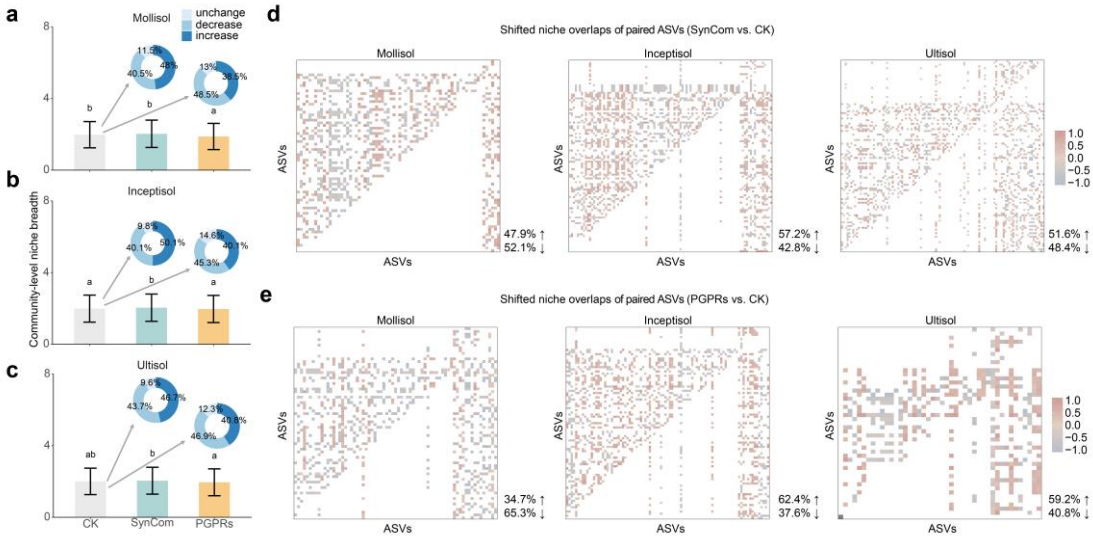

Figure S12 Niche breadth and overlap across three types of soils with different microbial inoculants. a-c, Changes in community-level niche breadth. Error bars represent the standard error. The different letters indicate significant differences ($P < 0.05$) using multiple comparisons of nonparametric tests (Nemenyi test). Pie charts show the proportion of increasing and decreasing niche breadths after inoculations compared with the control group (CK). **d** and **e** Shifted niche overlaps of paired ASVs that significantly increased or decreased ($P < 0.05$) in niche breadths after microbial inoculations. The differences were obtained by subtracting the niche breadths of ASVs after inoculations from those of the CK.

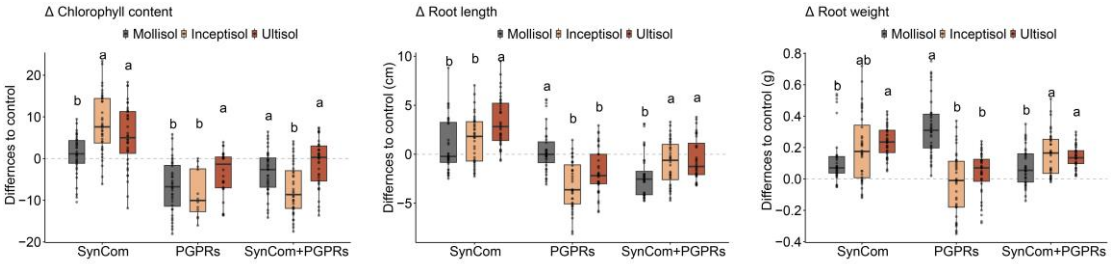

Figure S13 Morphological traits of maize grown in the double-tube chambers at day 15 between microbial inoculations and CK. n = 6 biological replicates of maize plants were evaluated, except for n = 2 and n = 5 for plants grown in Inceptisol and Ultisol with PGPR treatments, respectively. For the soil plant analysis development (SPAD) value, each plant was measured three times. The symbol of Δ represents the differences between inoculated and inoculated treatments. The different letters indicate significant differences ($P < 0.05$) using multiple comparisons of nonparametric tests (Nemenyi test). In box plots, the horizontal bars represent medians. The tops and bottoms of the boxes show the 75th and 25th percentiles, respectively.

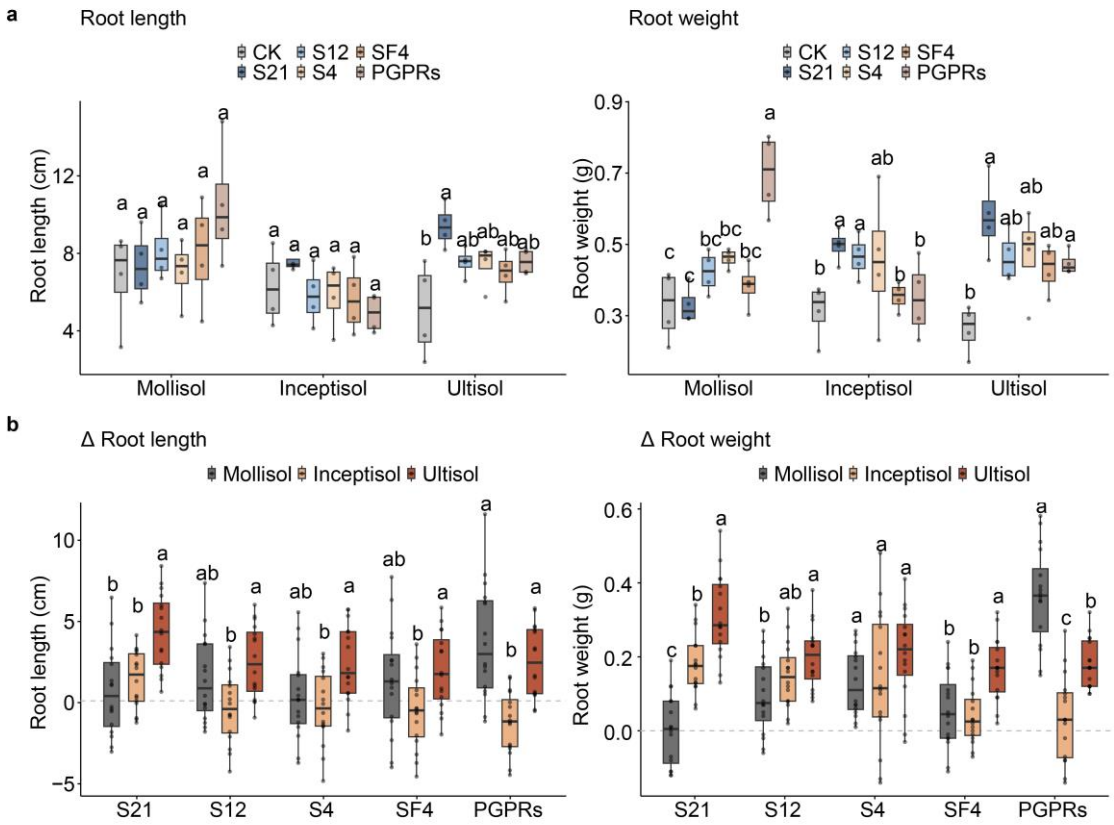

Figure S14 Root development of maize grown in the double-tube chambers at day 10 between microbial inoculations and CK. n = 4 biological replicates of maize plants were evaluated. S21, 21-species SynCom. S12, 12-species SynCom simplified at the genus level. S4,4-species SynCom simplified at the order level. SF4,4-species SynCom functionally similar to PGPRs. The symbol of Δ in **b** represents the differences between inoculated and inoculated treatments. The different letters indicate significant differences ($P < 0.05$) using multiple comparisons of nonparametric tests (Nemenyi test). In box plots, the horizontal bars represent medians. The tops and bottoms of the boxes show the 75th and 25th percentiles, respectively.

Supplementary Tables

Table S1 Ingredients of four selective medium to culture the native rhizosphere bacteria. All media were supplemented with amphotericin B (2 mg/mL) to prevent fungal growth.

	Ingredients	g/mL	Final pH
Medium #1	Casein tryptone	15	7.3 ± 0.2
	papain digest of soybean meal	5	
	Sodium chloride	5	
	Agar	15	
Medium #2	K_2HPO_4	3	6.8 ± 0.2
	NaH_2PO4	1	
	NH_4Cl	1	
	$MgSO_4 \cdot 7H_2O$	0.3	
	Agar	15	
	Cellobiose	10	
	L-Methionine	0.001	
	L-Glutamic acid	0.005	
	Cephalexin	0.01	
	Bacitracin	0.01	
Medium #3	Mannitol	10	6.8 ± 0.2
	K_2HPO_4	0.5	
	$MgSO_4$	0.2	
	Yeast extract	1	
	NaCl	0.1	
	Agar	20	
Medium #4	Trypticase soy agar	4	6.8 ± 0.2
	Yeast extract	2	
	NaCl	20	
	Methyl red	0.150	
	Agar	15	

Table S2 Plant growth-promoting traits of isolated microbial strains. GA: gibberellins, IAA: indole acetic acid, ACC: 1-aminocyclopropane-1-carboxylic acid, HCN: hydrogen cyanide. No specific plant-growth promoting traits of *Sphingomonas desiccabilis* have been studied, but it has been reported to be from biological soil crusts. The 12-species SynCom (S12) included *Acinetobacter pittii*, *Bacillus cereus*, *Chryseobacterium cucumeris*, *Citrobacter farmeri*, *Enterobacter cancerogenus*, *Klebsiella aerogenes*, *Lysinibacillus macroides*, *Pantoea ananatis*, *Pseudomonas mosselii*, *Serratia marcescens*, *Sphingomonas desiccabilis*, and *Stenotrophomonas rhizophila.* The 4-species SynCom (S4) included *Chryseobacterium cucumeris*, *Klebsiella aerogenes*, *Lysinibacillus macrolides*, and *Sphingomonas desiccabilis*. The asterisk (*) indicates that the ASVs shared 99% sequence identity with the isolates. The matching ASVs displayed >98.7% identity with the sequence of the full length of the 16S rRNA gene of each strain.

Number of isolates	Best hit taxonomy	Hit taxon name	Hit strain name	Accession	Similarity (%)	Completeness (%)	Potential for plant growth promotion	References	Matching ASVs
1	Bacteria; Proteobacteria; Gammaproteobacteria; Moraxellales; Moraxellaceae; Acinetobacter	*Acinetobacter calcoaceticus*	DSM 30006(T)	AIEC01000170	99.72	100	Phosphate solubilization Nitrogen fixation GA production	(Kang *et al.*, 2009; Peix *et al.*, 2009)	ASV7128
4	Bacteria; Proteobacteria; Gammaproteobacteria; Moraxellales; Moraxellaceae; Acinetobacter	*Acinetobacter pittii*	CIP 70.29(T)	APQP01000001	99.79	100	Phosphate solubilization	(Wan *et al.*, 2020)	ASV7128
1	Bacteria; Firmicutes; Bacilli; Bacillales; Bacillaceae; Bacillus	*Bacillus cereus*	ATCC 14579(T)	AE016877	99.79	100	Siderophore production Phosphate solubilization	(Lalloo *et al.*, 2010; Saeid *et al.*, 2018)	ASV33
1	Bacteria; Bacteroidetes; Flavobacteriia; Flavobacteriales; Weeksellaceae; Chryseobacterium	*Chryseobacterium cucumeris*	GSE06(T)	LUVZ01000011	99.22	100	Antimicrobial activity IAA production Phosphate solubilization Siderophore, urease, and ammonia production	(Jeong *et al.*, 2016)	ASV2426
1	Bacteria; Proteobacteria; Gammaproteobacteria; Enterobacterales; Enterobacteriaceae; Citrobacter	*Citrobacter farmeri*	CDC 2991-81(T)	AF025371	98.95	95.8	Phosphate solubilization	(Li *et al.*, 2022)	ASV859
2	Bacteria; Proteobacteria; Gammaproteobacteria; Enterobacterales; Enterobacteriaceae; Enterobacter	*Enterobacter cancerogenus*	ATCC 33241(T)	FYBA01000020	99.65	100	IAA production Phosphate solubilization Siderophore production	(Jha *et al.*, 2012)	ASV29

Number of isolates	Best hit taxonomy	Hit taxon name	Hit strain name	Accession	Similarity (%)	Completeness (%)	Potential for plant growth promotion ACC deaminase and ammonia	References	Matching ASVs
1	Bacteria; Proteobacteria; Gammaproteobacteria; Enterobacterales; Enterobacteriaceae; Enterobacter; Enterobacter hormaechei	*Enterobacter hormaechei subsp. steigerwaltii*	DSM 16691(T)	CP017179	99.72	100	Phosphate solubilization	(Gupta *et al.*, 2012)	ASV29
1	Bacteria; Proteobacteria; Gammaproteobacteria; Enterobacterales; Enterobacteriaceae; Enterobacter	*Enterobacter ludwigii*	EN-119(T)	JTLO01000001	99.3	100	Phosphate solubilization IAA production Siderophore production HCN production	(Shoebitz *et al.*, 2009; Yousaf *et al.*, 2011)	ASV29
1	Bacteria; Proteobacteria; Gammaproteobacteria; Enterobacterales; Enterobacteriaceae; Klebsiella	*Klebsiella aerogenes*	KCTC 2190(T)	CP002824	99.79	100	IAA production Phosphate solubilization	(Cheng *et al.*, 2022)	ASV29
1	Bacteria; Proteobacteria; Gammaproteobacteria; Enterobacterales; Enterobacteriaceae; Klebsiella; Klebsiella variicola	*Klebsiella pneumoniae subsp. rhinoscleromatis*	ATCC 13884(T)	ACZD01000038	99.16	100	IAA production Nitrogen fixation	(Chelius & Triplett, 2000)	ASV176
2	Bacteria; Proteobacteria; Gammaproteobacteria; Enterobacterales; Enterobacteriaceae; Klebsiella; Klebsiella variicola	*Klebsiella variicola subsp. tropica*	SB5531(T)	CAAHGN010000012	99.3	100	Nitrogen fixation IAA production Phosphate solubilization Siderophore production secondary metabolite synthesis	(Wyres *et al.*, 2020)	ASV176
1	Bacteria; Firmicutes; Bacilli; Bacillales; Planococcaceae; Lysinibacillus	*Lysinibacillus macroides*	DSM 54(T)	LGCI01000008	98.68	100	Nitrogen fixation	(Zhao *et al.*, 2022)	ASV8065

Number of isolates	Best hit taxonomy	Hit taxon name	Hit strain name	Accession	Similarity (%)	Completeness (%)	Potential for plant growth promotion	References	Matching ASVs
1	Bacteria; Proteobacteria; Gammaproteobacteria; Enterobacterales; Erwiniaceae; Pantoea	*Pantoea vagans*	LMG 24199(T)	EF688012	99.42	95.7	IAA production Phosphate solubilization	(Smits *et al.*, 2010; Mei *et al.*, 2021)	ASV6398*
3	Bacteria; Proteobacteria; Gammaproteobacteria; Pseudomonadales; Pseudomonadaceae; Pseudomonas	*Pseudomonas aeruginosa*	JCM 5962(T)	BAMA01000316	99.79	100	IAA and ACC deaminase production Phosphate solubilization	(Kothamasi *et al.*, 2006; Noreen *et al.*, 2012)	ASV1479
3	Bacteria; Proteobacteria; Gammaproteobacteria; Lysobacterales; Lysobacteraceae; Stenotrophomonas	*Pseudomonas geniculata*	ATCC 19374(T)	AB021404	99.93	97.1	Antifungal activity IAA and ACC deaminase production Phosphate solubilization	(Lau *et al.*, 2020)	ASV60
1	Bacteria; Proteobacteria; Gammaproteobacteria; Pseudomonadales; Pseudomonadaceae; Pseudomonas	*Pseudomonas koreensis*	Ps 9-14(T)	AF468452	99.37	100	Antifungal activity Nitrogen fixation IAA and cytokinin-like production	(Rafikova *et al.*, 2016)	ASV127
4	Bacteria; Proteobacteria; Gammaproteobacteria; Pseudomonadales; Pseudomonadaceae; Pseudomonas	*Pseudomonas mosselii*	CIP 105259(T)	AF072688	99.37	100	Phosphate solubilization IAA production Antifungal activity	(Naik *et al.*, 2008; Naik *et al.*, 2008)	ASV127
16	Bacteria; Proteobacteria; Gammaproteobacteria; Enterobacterales; Yersiniaceae; Serratia	*Serratia marcescens*	ATCC 13880(T)	JMPQ01000005	99.65	100	Phosphate solubilization	(Gupta *et al.*, 2012)	ASV30
1	Bacteria; Proteobacteria; Alphaproteobacteria; Sphingomonadales; Sphingomonadaceae; Sphingomonas	*Sphingomonas desiccabilis*	CP1D(T)	AJ871435	99.85	100			ASV4897*
1	Bacteria; Proteobacteria; Gammaproteobacteria; Lysobacterales; Lysobacteraceae; Stenotrophomonas	*Stenotrophomonas rhizophila*	QL-P4	CP016294	99.58	100	Antifungal activity IAA production	(Schmidt *et al.*, 2012)	ASV6550*

Number of isolates	Best hit taxonomy	Hit taxon name	Hit strain name	Accession	Similarity (%)	Completeness (%)	Potential for plant growth promotion	References	Matching ASVs
1	Bacteria; Proteobacteria; Gammaproteobacteria; Lysobacterales; Lysobacteraceae; Stenotrophomonas	*Stenotrophomonas maltophilia*	MTCC 434(T)	JALV01000036	98.95	100	Antimicrobial activity	(Ryan *et al.*, 2009)	ASV688

Table S3 Data quality of absolute quantification of the 16S rRNA gene.

RZ sample	No. of raw reads	Q20(%)	Q30(%)	No. of clean reads	Q20(%)	Q30(%)	Average length (bp)
Mollisols	2688498	98.0	96.2	2033806	99.1	98.0	
Inceptisols	2438076	98.0	96.1	435163	99.2	98.2	376.6
Ultisols	3015138	98.0	96.1	2662482	99.3	98.3	

RZ, rhizosphere. n = 6 for each soil.

Table S4 Physicochemical properties of rhizosphere samples. RZ, rhizosphere. n = 6 for each soil.

RZ sample	Moisture	NO_3^--N	NH_4^+-N	pH	SOM	Total N	Total P	Total K	Avail N	Avail P	Avail K
	%	mg/kg	mg/kg		g/kg	g/kg	g/kg	g/kg	mg/kg	mg/kg	mg/kg
Mollisols	26.65 ± 0.80a	7.7 ± 4.0a	6.1 ± 1.6	6.98 ± 0.07b	48 ± 2.2a	2.09 ± 0.05a	0.94 ± 0.10a	18.83 ± 1.3a	205.8 ± 20.8a	33.2 ± 10.6a	225.8 ± 51.6a
Inceptisols	16.65 ± 0.67b	7.1 ± 4.0ab	5.5 ± 1.6	8.61 ± 0.05a	10 ± 0.8c	0.62 ± 0.03c	0.79 ± 0.07b	17.43 ± 0.3b	52.68 ± 13.7b	3.4 ± 1.9b	108.3 ± 12.5b
Ultisols	16.68 ± 0.76b	3.2 ± 1.9b	5.0 ± 1.7	6.81 ± 0.13c	13 ± 1.5b	0.83 ± 0.06b	0.54 ± 0.06c	9.77 ± 0.3c	52.68 ± 7.6b	24.1 ± 9.8a	266.7 ± 30.3a

Table S5 Metagenomic datasets and assembly results. RZ, rhizosphere. n = 6 for each soil.

RZ sample	No. of total scaffolds	Total length (Mb)	N50 (bp)	N90 (bp)	Longest scaffolds (bp)	Average length (bp)
Mollisols	126678	104031324	777	534	79778	
Inceptisols	72437	55236317	734	531	28471	854.3
Ultisols	447269	429127627	978	549	60783	

Table S6 Genome bins retrieved from soil metagenomes. Bold font denotes contamination < 5%.

bin	Completeness (%)	Contamination (%)	GC	Lineage	Size	N50	Conserved genes
bin.13	98.6	1.6	0.60	Rhizobiaceae	5843771	112013	*rpoD*
bin.15	89.3	1.7	0.29	Parvibaculaceae	1161500	5426	*rpoD, 16 s*
bin.9	87.9	3.2	0.67	Micrococcaceae	3756813	11275	*rpoD, 5 s*
bin.8	86.2	4.0	0.69	Sphingomonadaceae	3828611	5911	*rpoD*
bin.25	83.1	1.3	0.66	Sphingomonadaceae	2370889	9357	*5s*
bin.20	79.7	3.6	0.69	Xanthomonadaceae	3990213	3782	*rpoD*
bin.11	75.8	1.7	0.71	Conexibacteraceae	1983021	3361	*rpoD, 16 s*
bin.7	72.3	9.1	0.64	Sphingomonadaceae	2352056	18012	-
bin.12	68.1	0.2	0.71	Gemmatimonadaceae	4435646	54434	*rpoD, 5 s, 16 s*
bin.16	59.3	0.4	0.70	Conexibacteraceae	1636268	4600	*rpoD*
bin.6	59.0	3.2	0.67	Burkholderiales	2537564	2724	*rpoD*
bin.27	54.2	8.6	0.69	Acidobacteriaceae	2190458	3400	*rpoD, 16 s*
bin.21	53.9	9.1	0.57	Nitrospiraceae	1666903	2922	*rpoD*
bin.26	53.7	7.3	0.69	Rubrobacteraceae	1589736	56822	*rpoD*
bin.14	51.4	9.0	0.52	Herpetosiphonaceae	2604078	3377	*rpoD, 23 s*
bin.18	51.3	7.3	0.58	Nitrospiraceae	1811438	4112	*rpoD*
bin.1	50.8	9.6	0.67	Nocardiaceae	3490541	2447	*rpoD*
bin.19	50.7	4.3	0.72	Frankiaceae	1806731	4415	*rpoD*
bin.2	50.6	6.9	0.71	Intrasporangiaceae	3442070	4256	-
bin.17	50.2	4.8	0.69	Sphingomonadaceae	1906645	2220	-
bin.22	50.1	1.5	0.64	Sphingomonadaceae	2101633	2420	*16s, 23 s*
bin.23	50.1	7.3	0.74	Rubrobacteraceae	3157192	20505	*rpoD*

Table S7 Parameters of the logistic model of SynCom and PGPRs. A1: initial value; A2: final value; p: maximum growth rate; x0: inflection point, the time of maximum growth rate. The t test was performed before the normal test. Only groups with statistically significant differences are marked. n = 4 for each group.

Formula	$y = A2 + (A1 - A2)/(1 + (x/x0)p)$	
	SynCom	PGPRs
A_1	0.02 ± 0.1	0.02 ± 0.23
A_2	2.48 ± 0.05b	3.95 ± 0.83a
x_0	16.97 ± 1.1	18.22 ± 7.8
p	3.4 ± 0.49a	1.1 ± 0.53b
R^2	97.7%	96.4%

Table S8 Alpha diversity of rhizosphere soils after treatment with SynCom and PGPRs. Up arrows indicate a significant increase compared to CK accordingly. n = 4 for each group.

	Richness index			Shannon index			Chao1 index		
	Greenhouse experiment after inoculate with								
	CK	PGPRs	SynCom	CK	PGPRs	SynCom	CK	PGPRs	SynCom
Mollisols	2022 ± 70	1904 ± 50	2017 ± 41	6.81 ± 0.03	6.72 ± 0.06	6.80 ± 0.03	2031 ± 68	1917 ± 49	2029 ± 42
Inceptisols	2117 ± 105	1939 ± 234	2043 ± 146	6.88 ± 0.08	6.82 ± 0.13	6.84 ± 0.08	2130 ± 106	1952 ± 234	2057 ± 144
Ultisols	342 ± 29	362 ± 25	859 ± 82↑	5.29 ± 0.08	5.04 ± 0.21	5.29 ± 0.05↑	346 ± 28	363 ± 25	863 ± 82↑

Table S9 Twelve primers used for qPCR analysis

ID	Name	Primer		Sequence (5' to 3')	Product (bp)
R5	*Bacillus cereus*	Primer 27	F	AGCAACGCGAAGAACCTTAC	234
			R	ATTTGACGTCATCCCCACCT	
C5	*Enterobacter cancerogenus*	Primer 28	F	TTCTTCATACACGCGGCATG	201
R6	*Enterobacter ludwigii*		R	CTCTTGCCATCAGATGTGCC	
R9	*Pseudomonas koreensis*	Primer 31	F	CGGATGAAAGGAGCTTGCTC	297
			R	CAATATTCCCCACTGCTGCC	
R11	*Chryseobacterium cucumeris*	Primer 33	F	GCGGTAGAGATCTTTCGGGA	261
			R	CCGTGTCTCAGTACCAGTGT	
R12	*Stenotrophomonas maltophilia*	Primer 34	F	AGGTGGTCGTTTAAGTCCGT	247
			R	CCAGTTCGCATCGTTTAGGG	
C6	*Lysinibacillus macroides*	Primer 42	F	ATTTGACGTCATCCCCACCT	212
			R	TCTTGACATCCCGTTGACCA	
A7	*Serratia marcescens*	Primer 44	F	TCACCGCTACACCTGGAATT	
A8	*Pantoea vagans*		R	GGCAGCAGTGGGGAATATTG	345
A9	*Citrobacter farmeri*				
C8	*Enterobacter hormaechei subsp. steigerwaltii*				
A5	*Stenotrophomonas rhizophila*	Primer 5	F	GTCTGTTGTGAAAGCCCTGG	233
			R	CCAGTTCGCATCGTTTAGGG	
C4	*Pseudomonas mosselii*	Primer 50	F	CGCGTAGGTGGTTCGTTAAG	270
			R	TCTCAAGGATTCCAACGGCT	
C15	*Acinetobacter pittii*	Primer 51	F	GCAGCAGTGGGGAATATTGG	319
			R	TCCTCTCCCACACTCTAGCT	
X1	*Pseudomonas geniculata*	Primer 10	F	AGGTGGTCGTTTAAGTCCGT	247
			R	CCAGTTCGCATCGTTTAGGG	
X2	*Sphingomonas desiccabilis*	Primer 11	F	CGACGATCCTTAGCTGGTCT	363
			R	CTCCTGGATTCAAGCGATGC	

Table S10 PERMANOVA test statistics of the influence of soil types and microbial inoculations on the soil community composition.

	Df	Sum of squares	R^2	F	Pr(>F)	
Soil type	2	6.9538	0.80302	50.8893	0.001	***
Microbial inoculation	2	0.173	0.01998	1.2662	0.249	
Soil type:Microbial inoculation	4	0.3029	0.03498	1.1085	0.376	
Residual	18	1.2298	0.14202			
Total	26	8.6596	1			

Formula = adonis2(ASV ~ Soil type*Microbial inoculation, data, permutations = 999, method="bray")

Supplementary methods

Methods S1

Solid-state ^{13}C nuclear magnetic resonance analysis

Hydrofluoric (HF) acid was used in a pretreatment step to prevent the interference of Fe^{3+} and Mn^{2+} ions in the soil before the solid-state ^{13}C NMR analysis of the soil samples. The specific steps of the methodology used were as follows: 5 g of air-dried soil sample was placed in a 100 mL plastic centrifugal tube, and 50 mL of HF acid solution (10% v/v) was added. Then, the tube was covered and shaken for 1 hour. The total mixture was centrifuged at 3000 r/min for 10 min, after which the supernatant was removed, and the residue continued to be treated with the HF acid solution. These steps were repeated 8 times, and the oscillation times were 1 hour (four times), 12 hours (three times), and 24 hours (one time). After being fully treated with the HF acid solution, the residue was washed with Milli-Q water 4 times to remove the remaining HF acid. The residue treated with HF acid was dried in an oven at 40 °C, ground through a 60-mesh sieve, and used in the NMR analysis. The HF acid-pretreated soil sample was subjected to solid-state magic-angle spinning NMR measurements (AVANCE II 300 MH). The chemical shift in the main ^{13}C signal of SOC corresponded to the following carbon structures (Huimin *et al.,* 2019): 0-45 ppm alkyl C, 65-95 ppm O-alkyl C, 95-110 ppm acetal C, 110-140 ppm aromatic C, and 160-220 ppm carbonyl C. The relative contents of the various carbon chemical components were obtained by regional integration of spectral peak curves.

Methods S2

Soil physical and chemical properties

The physicochemical properties of rhizosphere soils were determined as follows: Soil pH was determined using a glass electrode in a soil:water ratio of 1:2.5 (w/v). Soil organic matter was determined by the potassium dichromate oxidation method (Walkley & Black, 1934). Total nitrogen was determined by the semimicro Kjeldahl method, and nitrate (NO_3^--N) and ammonium nitrogen (NH_4^+-N) were extracted with 2 M KCl using a continuous flow analyzer (Lu, 2000). Available nitrogen was determined

by the alkaline hydrolysis diffusion method (Lu, 2000). Total phosphorus and available phosphorus were measured with the sodium carbonate and Olsen-P methods, respectively (Lu, 2000). Total potassium and available potassium were measured by flame photometry after extraction with sodium hydroxide and ammonium acetate, respectively (Hald & Mason, 1958).

Methods S3

Bacterial cultivation and isolation

The specific steps of the standard serial dilution culture method were as follows: 1 g of rhizosphere soil samples was preserved at -80 °C before being weighed into a conical flask with 9 mL of sterile water, after which the conical flask was covered and shaken for 15 min (30 °C, 200 rpm/min). Then, the soil suspensions were serially diluted to create a diversity gradient (10^{-1}, 10^{-2}, 10^{-3}, 10^{-4}, 10^{-5}, and 10^{-6}), and the supernatant was smeared onto four different types of nutrient media for isolation and culture (Table S3). After 2 to 4 days of cultivation at 30 °C, single colonies were picked and subcultured on nutrient agar to obtain pure isolates and then preserved on LB plates at 4 °C.

Methods S4

Identification of the isolated microbial strains

DNA extraction of rhizosphere soil microbes. Genomic DNA was extracted by centrifugation, precipitation, dissolution, ice bath, water bath, and washing according to the standard protocols of Shanghai Personal Gene Technology. The bacterial 16S rRNA gene was amplified by using primers 27F (5' -AGAGTTTGATCCTGGCTCAG-3') and 1492R (5' -CTACGGCTACCTTGTTACGA- 3'). The sample PCR system (50 μL) contained 5 μL 10x PCR buffer, 1 μL dNTP, 1.5 μL of each primer, 1 μL Taq polymerase (5 U/μL, TaKaRa, Dalian), 39 μL ddH2O, and 1.0 μL DNA template. Cycle conditions were as follows: predenaturation at 95 °C for 5 min, denaturation at 95 °C for 30 s, annealing at 58 °C for 30 s, and 72 °C for 90 s (a total of 35 cycles), and extension at 72 °C for 10 min. The amplified DNA was then visualized through agarose gel electrophoresis (1% agarose) and recovered using an AxyPrep DNA Gel Extraction

Kit (Axygen). The purified PRC products were sequenced by ABI3730-XL (Applied Biosystems, USA). The NCBI Blast program was employed to compare the sequence file with the data in the NCBI 16S rRNA database to obtain species identification based on the greatest sequence similarity.

Methods S5

IAA concentration of rhizosphere microbial communities

Detection of indole-3-acetic acid (IAA) produced by rhizosphere microbial communities was determined by means of the Salkowski reagent method (Sarwar & Kremer, 1995). One gram of rhizosphere soil was used to prepare 10 mL soil suspensions. The solutions were shaken well and allowed to stand for 15 min. Then, 0.5 mL of each supernatant was inoculated into 50 mL of liquid KB medium and incubated for 4 days for colorimetric IAA detection. Cell-free supernatant was mixed with Salkowski reagent (50.0 mM $FeCl_3$, 35.0% (v/v) perchloric acid) at a ratio of 3:2 and incubated for 30 min in the absence of light. The IAA concentration was measured at 530 nm and quantified using a standard curve.

Methods S6

Absolute quantification of 16S rRNA

First, DNA extraction of rhizosphere soil microbes was performed. Microbial genomic DNA was extracted from soil samples using a HiSeq Reagent Kit (Illumina, USA) in combination with the freeze-grinding method and purified by agarose gel electrophoresis. The concentration and purity of the extracted DNA were tested using a NanoDrop 2000 (Thermo Fisher Scientific, USA). The quality requirements were as follows: concentration ≥ 20 ng/μL, total ≥ 500 ng, $OD_{260/280}$ = 1.8-2.0. The DNA was stored at -20 °C for later use.

Second, target region detection and amplification. Spike-in sequences with conserved regions identical to those of natural 16S rRNA genes and variable regions replaced by random sequences with approximately 40% GC content were artificially synthesized. The V4-V5 regions of the 16S rRNA gene were amplified by PCR using 515F (5′-GTGCCAGCMGCCGCGG-3′) and 907R (5′-

CCGTCAATTCMTTTRAGTTT-3′). Agarose gel electrophoresis was used to determine whether the amplification products were single and specific. The sample PCR system (25 μL) contained 1x PCR buffer, 2.0 mM $MgCl_2$, 0.25 M dNTPs, 0.4 μM upstream and downstream primers, 1.5 U DNA polymerase (TaKaRa, Dalian) and 1.0 μL DNA template. The spike-in sequences involved conserved regions identical to selected natural 16S rRNA genes and artificial variable regions, working as internal standards and allowing absolute quantification across samples (Mou *et al.*, 2020). The PCR procedure involved predenaturation at 94 °C for 2 min, denaturation at 94 °C for 30 s, annealing at 55 °C for 30 s, and 72 °C for 60 s (a total of 25 cycles), and extension at 72 °C for 10 min. Agarose gel electrophoresis was used to determine whether the amplification products were single and specific. PCR products were purified with Agencourt AMPure XP (Beckman Coulter, USA) nucleic acid-purified magnetic beads.

Third, library quantification and pooling were performed. According to the preliminary quantitative results of the agarose gel electrophoresis, the samples with respective index labels were appropriately diluted, and then Qubit was used to precisely quantify the library. According to the sequencing flux requirements of different samples, the samples were mixed in proportion (molar ratio). The mixed library was detected with an Agilent 2100 Bioanalyzer (Agilent Technologies, USA) to determine the size of the inserted fragments of the sequencing library, confirm nonspecific amplification between 120 and 200 bp, and accurately quantify the concentration of the sequencing library. The library was sequenced using the Illumina NovaSeq 6000 Sequencer using the 2×250 bp paired-end method (Shanghai Genesky Biotechnologies Inc., Shanghai, China).

Finally, high-throughput sequencing data analysis was performed. TrimGalore (http://www.bioinformatics.babraham.ac.uk/projects/trim_galore/) and FLASH2 (Magoc & Salzberg, 2011) were used to process the final V4-V5 tag sequences. Only sequences >100 bp and those with an average score >20 were included for further analysis. The clean reads were clustered into a species-level taxon by standard threshold, and chimeras were removed by USEARCH (v10). The spike-in sequences were filtered

out, and reads were counted. The standard curve of spike-in sequences was generated for each sample, and the sequenced microbial DNA was quantified and estimated in reference to the representative standard curve. Taxonomic annotation was performed at a confidence threshold of 80% by Mothur (v1.41.1) with the command classify.seqs based on the RDP (v11.5) database (Cole *et al.*, 2013).

Methods S7

Relative quantification of 16S rRNA

The relative quantification of 16S rRNA, including DNA extraction of rhizosphere soil microbes, target region detection and amplification, library quantification and pooling, and high-throughput sequencing data analysis, was carried out as described above. Therefore, the specific steps of PCR were the same as absolute quantification without spike-in sequences.

Methods S8

Whole metagenomic shotgun sequencing

First, DNA extraction was performed as described above. The DNA concentration was measured by a NanoDrop 2000 (Thermo Fisher Scientific, USA), and its molecular size was estimated by agarose gel electrophoresis.

Second, DNA library construction and sequencing were performed. DNA libraries were constructed according to the manufacturer's instructions (Illumina). The same workflows from Illumina were used to perform cluster generation, template hybridization, isothermal amplification, linearization, blocking, denaturing and hybridization of the sequencing primers. Whole metagenomic shotgun sequencing was performed using the Illumina HiSeq 2500 sequencer using the 2×150 bp paired-end method (Shanghai Genesky Biotechnologies Inc., Shanghai, China). Low-quality reads (reads containing adaptor sequences, length of short reads < 100 bp, reads with error rate > 2, reads where ≥ 90% of the bases ≤ 20 bp) were removed.

Third, de novo assembly of the Illumina short reads was performed. Clean reads were assembled into scaffolds by SOAPdenovo (version 1.05) with different k-mers, which was based on De-Brujin graph construction. Scaffolds were preserved for further

analysis only when they were longer than 500 bp and had greater N50 scores. Open reading frames (ORFs) were predicted by MetaGeneMark (version 2.10) (Zhu *et al.*, 2010). The clusters of genes (identity > 95%, coverage > 90%) and nonredundant gene sets were achieved by CD-HIT. The predicted genes were further annotated functionally by the BLAST program (Version 2.2.28+) against KEGG (Kyoto Encyclopedia of Genes and Genomes). According to the KO annotation information, the KO abundances of each metabolic pathway at Level 1, Level 2 and Level 3 were accumulated for each sample.

Finally, metagenomic binning and qualification were performed. Assembled scaffolds were then grouped into metagenomic bins using MetaWRAP (Uritskiy *et al.*, 2018). Genome bins were assessed for estimated completeness and contamination markers by CheckM (Parks *et al.*, 2015). The completeness and contamination can be estimated by the number of single-copy genes that the genome of the bin's taxonomy is expected to have. Genome bins were filtered to > 50% completeness and < 10% contamination. Binned genomes were submitted to the RAST server for classification and annotation of nutrient metabolism, plant hormone synthesis pathways, bacterial motility and chemotaxis (Aziz *et al.*, 2008; Overbeek *et al.*, 2014; Brettin *et al.*, 2015).

References

Aziz RK, Bartels D, Best AA, DeJongh M, Disz T, Edwards RA, Formsma K, Gerdes S, Glass EM, Kubal M, Meyer F, Olsen GJ, Olson R, Osterman AL, Overbeek RA, McNeil LK, Paarmann D, Paczian T, Parrello B, Pusch GD, Reich C, Stevens R, Vassieva O, Vonstein V, Wilke A, Zagnitko O. 2008. The RAST Server: rapid annotations using subsystems technology. *BMC Genomics* **9**: 75.

Brettin T, Davis JJ, Disz T, Edwards RA, Gerdes S, Olsen GJ, Olson R, Overbeek R, Parrello B, Pusch GD, Shukla M, Thomason JR, Stevens R, Vonstein V, Wattam AR, Xia F. 2015. RASTtk: a modular and extensible implementation of the RAST algorithm for building custom annotation pipelines and annotating batches of genomes. *Scientific Reports* **5**: 8365.

Chelius MK, Triplett EW. 2000. Immunolocalization of dinitrogenase reductase produced by *Klebsiella pneumoniae* in association with *Zea mays* L. *Applied and Environmental Microbiology* **66**(2): 783-787.

Cole JR, Wang Q, Fish JA, Chai B, McGarrell DM, Sun Y, Brown CT, Porras-Alfaro A, Kuske CR, Tiedje JM. 2013. Ribosomal database project: Data and tools for high throughput rRNA analysis. *Nucl Acids Res* **42**(D1): D633-D642.

Gupta M, Kiran S, Gulati A, Singh B, Tewari R. 2012. Isolation and identification of phosphate solubilizing bacteria able to enhance the growth and aloin-A biosynthesis of *Aloe barbadensis* Miller.

Microbiological Research **167**(6): 358-363.

Hald PM, Mason WB. 1958. Sodium and Potassium by flame photometry. *Standard Methods of Clincial Chemistry* **2**: 165-185.

Huimin S, Jiang J, Lina C, Wenting F, Yugang W, Jinchi Z. 2019. Soil organic carbon stabilization mechanisms in a subtropical mangrove and salt marsh ecosystems. *Science of the Total Environment* **673**: 502-510.

Kothamasi D, Kothamasi S, Bhattacharyya A, Kuhad RC, Babu CR. 2006. Arbuscular mycorrhizae and phosphate solubilizing bacteria of the rhizosphere of the mangrove ecosystem of Great Nicobar Island, India. *Biology and Fertility of Soils* **42**(4): 358-361.

Lau ET, Tani A, Khew CY, Chua YQ, Hwang SS. 2020. Plant growth-promoting bacteria as potential bioinoculants and biocontrol agents to promote black pepper plant cultivation. *Microbiological Research* **240**: 126549.

Lu R 2000. Analytical methods of soil agrochemistry.In. Beijing: China Agricultural Science and Technology Press.

Magoc T, Salzberg SL. 2011. FLASH: fast length adjustment of short reads to improve genome assemblies. *Bioinformatics* **27**(21): 2957-2963.

Mei C, Chretien RL, Amaradasa BS, He Y, Turner A, Lowman S. 2021. Characterization of phosphate solubilizing bacterial endophytes and plant growth promotion in vitro and in greenhouse. *Microorganisms* **9**(9): 1935.

Mou J, Li Q, Shi W, Qi X, Song W, Yang J. 2020. Chain conformation, physicochemical properties of fucosylated chondroitin sulfate from sea cucumber *Stichopus chloronotus* and its in vitro fermentation by human gut microbiota. *Carbohydrate Polymers* **228**: 115359.

Naik PR, Raman G, Narayanan KB, Sakthivel N. 2008. Assessment of genetic and functional diversity of phosphate solubilizing fluorescent pseudomonads isolated from rhizospheric soil. *BMC Microbiology* **8**: 230.

Naik PR, Sahoo N, Goswami D, Ayyadurai N, Sakthivel N. 2008. Genetic and functional diversity among fluorescent pseudomonads isolated from the rhizosphere of banana. *Microbial Ecology* **56**(3): 492-504.

Noreen S, Ali B, Hasnain S. 2012. Growth promotion of *Vigna mungo* (L.) by *Pseudomonas* spp. exhibiting auxin production and ACC-deaminase activity. *Annals of Microbiology* **62**(1): 411-417.

Overbeek R, Olson R, Pusch GD, Olsen GJ, Davis JJ, Disz T, Edwards RA, Gerdes S, Parrello B, Shukla M, Vonstein V, Wattam AR, Xia F, Stevens R. 2014. The SEED and the Rapid Annotation of microbial genomes using subsystems technology (RAST). *Nucleic Acids Research* **42**(Database issue): D206-D214.

Parks DH, Imelfort M, Skennerton CT, Hugenholtz P, Tyson GW. 2015. CheckM: assessing the quality of microbial genomes recovered from isolates, single cells, and metagenomes. *Genome Research* **25**(7): 1043-1055.

Rafikova GF, Korshunova TY, Minnebaev LF, Chetverikov SP, Loginov ON. 2016. A new bacterial strain, *Pseudomonas koreensis* IB-4, as a promising agent for plant pathogen biological control. *Microbiology* **85**(3): 333-341.

Ryan RP, Monchy S, Cardinale M, Taghavi S, Crossman L, Avison MB, Berg G, van der Lelie D, Dow JM. 2009. The versatility and adaptation of bacteria from the genus *Stenotrophomonas*. *Nature Reviews Microbiology* **7**(7): 514-525.

Sarwar M, Kremer RJ. 1995. Determination of bacterially derived auxins using a microplate method.

Letters in Applied Microbiology **20**(5): 282-285.

Schmidt CS, Alavi M, Cardinale M, Müller H, Berg G. 2012. *Stenotrophomonas rhizophila* DSM14405T promotes plant growth probably by altering fungal communities in the rhizosphere. *Biology and Fertility of Soils* **48**(8): 947-960.

Smits TH, Rezzonico F, Kamber T, Goesmann A, Ishimaru CA, Stockwell VO, Frey JE, Duffy B. 2010. Genome sequence of the biocontrol agent *Pantoea vagans* strain C9-1. *Journal of Bacteriology* **192**(24): 6486-6487.

Uritskiy GV, DiRuggiero J, Taylor J. 2018. MetaWRAP-a flexible pipeline for genome-resolved metagenomic data analysis. *Microbiome* **6**(1): 158.

Walkley A, Black IA. 1934. An examination of the Degtjareff method for determining soil organic matter, and a proposed modification of the chromic acid titration method. *Soil Science* **37**(1): 29-38.

Wyres KL, Lam M, Holt KE. 2020. Population genomics of *Klebsiella pneumoniae*. *Nature Reviews Microbiology* **18**(6): 344-359.

Zhao D, Jiao J, Du B, Liu K, Wang C, Ding Y. 2022. Volatile organic compounds from *Lysinibacillus macroides* regulating the seedling growth of *Arabidopsis thaliana*. *Physiology and Molecular Biology of Plants* **28**(11-12): 1997-2009.

Zhu W, Lomsadze A, Borodovsky M. 2010. Ab initio gene identification in metagenomic sequences. *Nucleic Acids Research* **38**(12): e132.